INSTANTANEOUS PRESSURE DISTRIBUTION AROUND A SPHERE IN UNSTEADY FLOW

Leslie S. G. Kovasznay, Itiro Tani, Masahiko Kawamura and Hajime Fujita

Department of Mechanics
The Johns Hopkins University

December 1971

Office of Naval Research
Washington D. C. 20360

Technical Report: ONR No. N00014-67-0163-002. Distribution of this document is unlimited. The findings of this report are not to be construed as an official Department of Navy position unless so designated by their authorized documents.

INSTANTANEOUS PRESSURE DISTRIBUTION AROUND A SPHERE IN UNSTEADY FLOW

Leslie S. G. Kovasznay, Itiro Tani, Masahiko Kawamura and Hajime Fujita

Department of Mechanics
The Johns Hopkins University

December 1971

Technical Report: ONR No. N00014-67-0163-002. Distribution of this document is unlimited.

ABSTRACT

In order to study effects of velocity and acceleration of a flow to the pressure on an obstacle, a small sphere with a pressure hole was placed in a periodically pulsating jet. Both the instantaneous pressure on the sphere and the instantaneous velocity of the flow field when the sphere was absent were measured. By using periodic sampling and averaging techniques, only periodic or deterministic component of the signal was recovered and any random component caused by turbulence suppressed. The measured surface pressure was expressed in terms of this measured velocity and acceleration of the flow. A simple inviscid theory was developed and the experimental results were compared with it.

ACKNOWLEDGEMENTS

This research was supported by U. S. Office of Naval Research under contract No. N00014-67-0163-0002.

The authors would like to express thanks to Mr. L. T. Miller for help in technical aspect, and to Mrs. C. L. Grate for the typing of the text.

TABLE OF CONTENTS

LIST OF ILLUSTRATIONS

1. INTRODUCTION

Measurement of the instantaneous value of the static pressure inside a turbulent flow is still an unresolved problem because the pressure probe placed in the unsteady flow field represents a solid boundary and the surface pressure at a point always contains important contributions from the inertial effects in the flow around the body. For steady flows it is relatively easy to design "static" probes that read the static pressure by using potential theory to calculate the pressure distribution around the body of the probe, but the same locations do not give instantaneous static pressure in unsteady flow.

In order to understand better the behavior of small probes placed in unsteady flows, an experiment was performed in a relatively simple configuration. A small sphere was placed in a pulsating jet and the instantaneous surface pressure fluctuations were measured. Since in such a flow there is a strong random component of fluctuations due to the turbulence, a special signal processing technique, namely periodic sampling and averaging was performed on all signals in order to enhance the periodic (or deterministic) component and to suppress the random component.

Furthermore, in order to provide a guide for the assessment of the results a simple inviscid theory was developed and the experimental results were compared with it.

2. EXPERIMENTAL FACILITY AND PROCEDURE

The time-dependent flow for measurements, the pulsating flow, is produced by the scheme indicated in Fig. 1. The steady air flow provided by the centrifugal blower is divided into two streams, the one flowing through the duct D_1 and the other through the duct D_2. One flow component is discharged through the duct D_1 and is periodically intercepted by a rotating disc with 16 holes. As a result periodic pressure fluctuations are induced also in the other branch, D_2, through which the other flow component is discharged and pulsating air jet is produced. The frequency and amplitude of the velocity fluctuation in the jet can be varied within limits varying the speed of the rotating disc and the stand-off between the disc and the nozzle attached to D_1.

The pulsating velocity of the jet was measured by a constant temperature hot-wire anemometer [1] followed by a linearizer. [2] Since hot-wire signal as obtained from the output of the linearizer still contains random fluctuations due to turbulence in the jet, special signal processing technique, periodic sampling and averaging, was performed by using "Wavefrom Eductor" Model TDH9 of Princeton Applied Research. The output of that instrument gives the ensemble average of a large number (typically 1000 - 2000) of sweeps and the random component is correspondingly reduced by a factor of $\sqrt{1000}$ $\sqrt{2000}$ or 30-40. As the result most of the random components is

suppressed and only periodic or deterministic component is recovered. The necessary synchronizing pulses were obtained from the rotating disc by using a photo-cell pick up. Fig. 2 shows an example of the periodic velocity fluctuation measured at a distance $x = 6$ cm from the nozzle at a pulsating frequency of $f = 450$ Hz. The same technique was used to obtain the periodic pressure fluctuation on the sphere as described below. Schematic diagram of the instrumentation is shown in Fig. 3.

Three spheres of the same diameter but with a pressure hole at different locations along the meridian were used as models. They are designated as S, O and R as shown in Fig. 4. The diameter of the sphere is 6.35 mm and the diameter of the pressure hole is 0.5 mm, located at the meridian angle $\theta = 0^{\circ}$ (opposite stem), 45° and 90° for S, O, and R respectively. The pressure hole is connected to a frequency modulated condenser microphone through the stem as shown in Fig. 4, and the pressure fluctuations is converted to the electrical signal. In earlier period of the experiment a transistiorized version of the circuit used by Einstein and Li [1] was used as the FM oscillator and the detector. In later period an improved circuit with the carrier frequency within the range of commercial FM broadcast was built into the probe as shown in Fig. 4 and an FM receiver EICO CORTINA 3200 was used as the detector.

The sphere was rotated around its center by a lathe turn table up to a maximum angle of $\pm$ 20° (Fig. 5) so by using all three models it

was possible to orient the pressure holes on the sphere at every 5° between -20° to 110°. The overall static sensitivity was found to be 57 and 2.4 $\mu V/\mu bar$ respectively. The overall frequency characteristics of the pressure probe depends on the diameter and length of the pipe leading to the microphone as well as on the volume of the cavity in front of the microphone diaphragm. Fig. 6 shows the calculated frequency characteristics for the combination of a pipe of diameter 1.0 mm and length 20.5 mm and for two values of the cavity of volume 1.65 and 89.1 mm^3, respectively. Resonances occur around 800 Hz and 2500 Hz respectively. The dynamic sensitivity of the probe would have been best obtained by the Coupler Method, which is based on a comparison with a standard microphone. Unfortunately, however, no standard microphone was available, so an alternative procedure was used by utilizing a theoretical relation obtained for a sphere. According to the theoretical calculation given in a later section, the pressure fluctuation on a sphere is made up of two terms, one being proportional to the fluctuating velocity itself and the other one proportional to the time derivative of the fluctuating velocity. At the forward stagnation point the non-dimensional coefficients of the two terms calculated by the theory are 1.0 and 1.5 respectively. By assuming a phase lag in the measured pressure fluctuation due to the lead pipe and the cavity volume, the ratio of the two coefficients, dynamic sensitivity, for the stagnation point was calculated as described in the following chapter from the fluctuating velocity and its time derivative obtained by a hot-wire placed at the location of the sphere center but in the absence of the sphere. The phase lag so determined

varied between 1^{o} and 30^{o}, and the dynamics sensitivity was found to be 10% - 40% higher than the static sensitivity.

3. EXPERIMENTAL RESULTS

First measurements were made within the jet which is discharged from the duct D_2 through a contracting nozzle to the ambient air (Fig. 1), for a mean velocity of about 20 m/s at the jet axis. Fig. 7 shows the velocity distribution across the steady non pulsating jet at two stations, $x = 3$ and 6 cm downstream from the nozzle. The core of the jet, defined as the region in which the velocity is greater than 90% of the velocity on the axis U_o has a diameter 1.55 cm at $x = 3$ cm and 1.28 cm at 6 cm, respectively. Fig. 8 shows the instantaneous velocity profiles across the fluctuating jet at a station $x = 5$ cm for a frequency of 450 Hz. The core diameter defined as above is about 1.20 cm, which is a little less than that of the steady jet. Fig. 9 shows the streamwise variation of the amplitude and phase velocity of the velocity fluctuation along the jet axis. Circles are described to indicate the location and size of the sphere. When the sphere is placed at $x = 3$ cm, the ratio of the core diameter of the steady jet to the sphere diameter is 2.4, but the amplitude of velocity fluctuation still varies by about 30 per cent over the region occupied by the sphere. When the sphere is placed at $x = 6$ cm, the ratio of the diameters is reduced to 2.0, but the variation of the amplitude of the velocity fluctuation becomes negligible. The phase velocity determined by two-hot wires separated by a fixed streamwise distance is approximately

constant over the region covered by experiment. The actual value was 13.2 m/s, about two thirds of the mean velocity at the jet axis. The phase velocity is regarded as the velocity of the travelling vortex ring produced at the nozzle traveling downstream.

Fig. 10 shows the mean (D. C.) pre sure distribution on the sphere placed at x = 3 cm in the steady jet. The calculated value are also shown. The Reynolds number based on the sphere diameter and the velocity on the axis is $\frac{U_0 a}{\nu} = 8.8 \times 10^3$. As shown later in the theory, the instantaneous surface pressure at a point can be expressed as

$$P = P_0 + A \frac{\rho}{2} U^2 + B \rho a \frac{dU}{dt}$$

where U is the instantaneous streamwise velocity component, a is the diameter of the sphere, A and B are the coefficients of the contribution from the instanteaneous velocity and from the instantaneous acceleration respectively.

The coefficients A and B are strong functions of the coordinates (the azimuth angle) and they may also weakly depend on the Reynolds number.

For the periodically pulsating flow, the above equation can be written more specifically as

$$P'(\tau) = A \frac{U^2(\tau)}{2} + B a \dot{U}(\tau)$$

where $P' = (P - P_0)/\rho$, $\tau = t/T$, T = Period

$$\dot{U} = \frac{dU}{dt}$$

for a particular location on the sphere. After the periodic sampling and averaging, values of all of $p'(\tau)$, $U^2(\tau)$ and $\dot{U}(\tau)$ were

sampled at ten equally spaced points over the entire period, and the coefficient A and B were determined by the method of least square so that the mean square error

$$\sum_{i=1}^{10} \left[p(\tau_i) - \left(\frac{A}{2} U^2(\tau_i) + Ba\dot{U}(\tau_i) \right) \right]^2$$

becomes minimum.

Fig. 11 to 14 show the experimental values of A and B, the two coefficients of influence. The values determined on the three models S, O and R are indicated in these figures by the symbols of square, circle and triangle, respectively. Solid curves give the theoretical prediction based on the assumption of inviscid irrotational flow described in the following chapter.

4. THEORY

With a view to gaining an insight into the problem, a theory is developed to predict the pressure acting on a sphere placed in a time-dependent flow of an inviscid fluid. A solution of the problem relevant to the subject was treated by Lamb[4] as follows. The pressure p on a sphere moving with time-dependent velocity V in an infinite mass of fluid at rest at infinity is given as

$$\frac{p - p_0}{\rho} = \left(-\frac{5}{4} + \frac{9}{4} \cos^2\vartheta \right) \frac{V^2}{2} - \frac{1}{2} \cos\vartheta \cdot a \frac{dV}{dt} \qquad (1)$$

where p_0 is the pressure at infinity, t the time, ρ the density of fluid, a the radius of the sphere, and ϑ the meridian angle measured from the rear stagnation point. Unfortunately, however, the problem treated there does not exactly correspond to the present experiment, since the time-

dependent flow that can be readily produced in the laboratory is a steady uniform flow with superimposed traveling disturbances with no associated pressure fluctuations in the free stream.

It is not difficult to illustrate the possibility of such a time-dependent flow. With the Cartesian coordinates (X, Y, Z), for example, the momentum equations are satisfied by taking a flow field

$$V_x = U_o, \quad V_y = f(x-U_o t), \quad V_z = 0, \quad \rho = \text{constant}, \qquad (2)$$

which represent a steady flow of velocity U_o on which a two-dimensional traveling disturbance is superimposed. No change in pressure is produced by the disturbance. Since, however, the disturbance is rotational having a component of vorticity in z-direction, the vortex filaments are stretched by the introduction of a three-dimensional body such as a sphere. This means that the "compensating flow" introduced to satisfy the boundary conditions on the sphere must be also be rotational. It does not seem to be impossible to find such a compensating flow, but in view of the limited range of application of the present theoretical calculation, it is doubtful whether the solution warrants the extra complication involved.

In order to simplify the calculations it is assumed that the disturbance is fufficiently small, irrotational and traveling with a velocity equal to that of the steady uniform flow. Using spherical polar coordinates (r, ϑ, λ) such that

$$X = r\cos\vartheta, \quad Y = r\sin\vartheta\cos\lambda, \quad Z = r\sin\vartheta\sin\lambda, \qquad (3)$$

the velocity potential is assumed in the form

$$\Phi = \Phi_0 + \Phi_1 + \Phi_2 \qquad (4)$$

where

$$\Phi_0 = U_0 r \left(1 + \frac{1}{2} \frac{a^3}{r^3} \right) \cos\vartheta \qquad (5)$$

is the velocity potential for the steady flow of velocity U_0 past a sphere of radius a with center at origin. The second term

$$\Phi_1 = \epsilon a U_0 \sin k(r\cos\vartheta - U_0 t)\, I_0(kr\sin\vartheta) \qquad (6)$$

is the velocity potential for the superimposed disturbance traveling with the phase velocity U_0 and wave number k, and finally

$$\Phi_2 = \epsilon a U_0 \sum_{n=1}^{\infty} C_n \frac{a^{n+1}}{r^{n+1}} P_n(\cos\vartheta) \qquad (7)$$

is the velocity potential for the compensating flow, ϵ is a non-dimensional constant, I_0 is the modified Bessel function of the first kind, P_n the Legendre polynomial of order n, and C_n the non-dimensional constants (n = 1, 2, 3, . . .) to be determined by applying the boundary conditions on the sphere. If ϵ is assumed to be small compared to unity, the disturbance represented by Φ_1 gives a velocity fluctuation of order $\epsilon k a U_0$ for finite values of $kr\sin\vartheta$, and, when superimposed on the steady uniform flow, produces a change in static pressure of order $\epsilon^2 k^2 a^2 \rho U_0^2$ which is second order and is considered negligible. Although the velocity fluctuation increase indefinitely as $kr\sin\vartheta$ tends to infinity, this does not seem to affect seriously the results provided that the consideration is limited to the region close to the sphere and an additional assumption is made that ka is small compared to unity, namely, the radius of the sphere is small compared to the wavelength of the disturbance. Fig. 15 shows the instantaneous streamlines (with equi-distant values of the Stokes stream function Ψ_1) for the velocity potential Φ_1 for a value $\epsilon = ka = 1/\sqrt{10}$

Under the assumption that ka is small, the normal velocity produced by the disturbance on the sphere is given by expanding eq. (6) and keeping the first two terms

$$\left(\frac{\partial \Phi_1}{\partial r}\right)_{r=a} = \varepsilon k a U_0 \left\{\cos\vartheta \cos k U_0 t + \frac{1}{2} ka(3\cos^2\vartheta - 1)\sin k U_0 t\right\}$$

which must be cancelled by the normal velocity calculated from $(\partial \Phi_2/\partial r)_{r=a}$. The constants in the expression for Φ_2 are then determined as

$$C_1 = \frac{1}{2} ka \cos k U_0 t, \quad C_2 = \frac{1}{3} k^2 a^2 \sin k U_0 t, \quad C_3 = C_4 = \cdots\cdots = 0$$

The pressure on the sphere is obtained from the equation

$$\frac{p}{\rho} + \frac{1}{2} q^2 + \frac{\partial \Phi}{\partial t} = F(t) \tag{8}$$

where

$$q^2 = \left(\frac{1}{r}\frac{\partial \Phi_0}{\partial \vartheta}\right)^2_{r=a} + \left(\frac{1}{r}\frac{\partial \Phi_1}{\partial \vartheta}\right)^2_{r=a} + \left(\frac{1}{r}\frac{\partial \Phi_2}{\partial \vartheta}\right)^2_{r=a}$$

$$= \frac{9}{4} U_0^2 \sin^2\vartheta \left\{1 + 2\varepsilon ka\left(\cos k U_0 t + \frac{5}{3} ka \cos\vartheta \sin k U_0 t\right\}\right.$$

$$\frac{\partial \Phi}{\partial t} = \left(\frac{\partial \Phi_1}{\partial t}\right)_{r=a} + \left(\frac{\partial \Phi_2}{\partial t}\right)_{r=a}$$

$$= -\varepsilon k a U_0^2 \left\{\cos k U_0 t + \frac{3}{2} ka \cos\vartheta \sin k U_0 t\right\}$$

$$F(t) = \frac{p_0}{\rho} + \frac{1}{2} U_0^2$$

p_0 being the pressure at infinity. The pressure on the sphere is thus given by

$$\frac{p - p_0}{\rho} = \frac{1}{2} A U_0^2 (1 + 2\varepsilon ka \cos k U_0 t) - B\varepsilon k^2 a^2 U_0^2 \sin k U_0 t \tag{9}$$

where

$$A = \frac{1}{4}(-5 + 9\cos^2\vartheta), \qquad B = \frac{3}{4}\cos\vartheta(3 - 5\cos^2\vartheta) \tag{10}$$

If the velocity V and the acceleration dV/dt at the location of the sphere center (r = o) are introduced by

$$\left.\begin{aligned} V &= U_0 + \left(\frac{\partial \Phi_1}{\partial x}\right)_{r=0} = U_0(1 + \varepsilon ka \cos k U_0 t) \\ \frac{dV}{dt} &= -\varepsilon k^2 a U_0^2 \sin k U_0 t \end{aligned}\right\} \tag{11}$$

the pressure on the sphere is expressed in the form

$$\frac{p-p_0}{\rho} = A\frac{V^2}{2} + Ba\frac{dV}{dt} \tag{12}$$

Eq. (12) indicates that the pressure on the sphere consists of two terms, the one being proportional to the instantaneous dynamic pressure $(1/2)\rho V^2$, and the other proportional to the time derivative of velocity $\rho a(dV/dt)$. The coefficient A of the first term is the same as for the classical solution (1), but the coefficient B of the second term is considerably different.

On writing

$$\vartheta = \pi - \theta \quad , \quad V = U_0 + u \tag{13}$$

where θ is the meridian angle measured from the forward stagnation point, and u is the velocity fluctuation, (12) and (10) are written in the form

$$\left.\begin{aligned} &\frac{p-p_0}{\rho} = A\frac{U_0^2}{2} + AU_0u + Ba\frac{du}{dt} \\ &A = \frac{1}{4}(-5+9\cos^2\theta) \quad , \quad B = \cos\theta(-3+5\cos^2\theta) \end{aligned}\right\} \tag{14}$$

5. DISCUSSION

In the theoretical calculation it was assumed that ε and ka are small compared to unity, namely, the amplitude of velocity fluctuation is small compared to the mean velocity on the jet axis, and the radius of sphere is small compared to the wavelength of velocity fluctuation. These conditions were not exactly satisfied in the experiment, where the maximum values of ε and ka are 0.40 and 0.68, respectively. Moreover, the observed phase velocity of velocity fluctuation was only 2/3 of the mean velocity, whereas in the theory the phase velocity is assumed to be equal

to the mean velocity.

In spite of these circumstances, however, the experimental values of the coefficients A and B agree fairly well with theoretical results for the sphere location at $x = 6$ cm (Figs. 13 and 14). The agreement is not as good for the location at $x = 3$ cm (Figs. 11 to 12), and this may be due to the undesirable variation of the velocity fluctuation amplitude around that location.

As seen from Fig. 2, the observed velocity fluctuation is not exactly simple sinusoidal, but a slight distortion in the wave form is apparent that results in higher harmonics. The distortion increases as the fundamental frequency decreases. This seems to account for the fact that the root-mean-square residual error of representing the observed pressure fluctuation by two terms amounts to 10.2, 9.7 and 6.9 per cent of the fluctuation amplitude for the fundamental frequency $f = 300$ Hz ($x = 3$ cm), 350 Hz ($x = 6$ cm) and 450 Hz ($x = 3$ and 6 cm), respectively.

No measurement on pressure was made on the rear side of the sphere, where the separation of flow is expected to modify the pressure distribution. The effect of separation can be traced in the pressure distribution for meridian angle greater than $\theta = 70^{\circ}$, where the experimental value of A begins to deviate from the theoretical curve (Figs. 13 and 14). On the other hand, the experimental value of B agrees fairly well with the theoretical result up to as far as $\theta = 90^{\circ}$ (Figs. 13 and 14). It is not certain whether the agreement is real or fortuitous.

6. CONCLUSIONS

Measurements of the instantaneous values of the surface pressure were carried out on a small sphere in a periodic pulsating flow and the experimental values agreed moderately well with a concurrently developed inviscid theory. It is apparent from the above theoretical and experimental work that similar calculations can be performed on bodies other than spheres or even on a combination of bodies. By judicious choice of such bodies points may be found on the surface where the coefficients $A = B = 0$ so the measured pressure has no contribution from the acceleration. Pressure transducers at such points or appropriately coupled to pressure holes at such points would indicate static pressure fluctuations in the flow corresponding to the location of the body but with the body absent quite similarlrly to static probes used in steady flows. The principal difference is that two terms must be cancelled instead the usual one in steady flow.

REFERENCES

1. Kovasznay, L. S. G. , Miller, L. T. and Vasudeva, B. R. (1963) A Simple Hot-Wire Anemometer, Project Squid Ted. Rep. JHU-22-P, Dept. of Aerospace Engr., Univ. of Virginia.

2. Kovasznay, L. S. G., and Chevray, R. (1969) Temperature Compensated Linearizers for Hot-Wire Anemometer, Rev. Sci. Inst., Vol. 40, p. 91.

3. Einstein, H. A. and Li, H. (1956) The Viscous Sublayer along a Smooth Boundary, Proc. Am. Soc. Civ. Engr. Paper 945.

4. Lamb, H. (1945) Hydrodynamics 6th ed., p. 124, Dover.

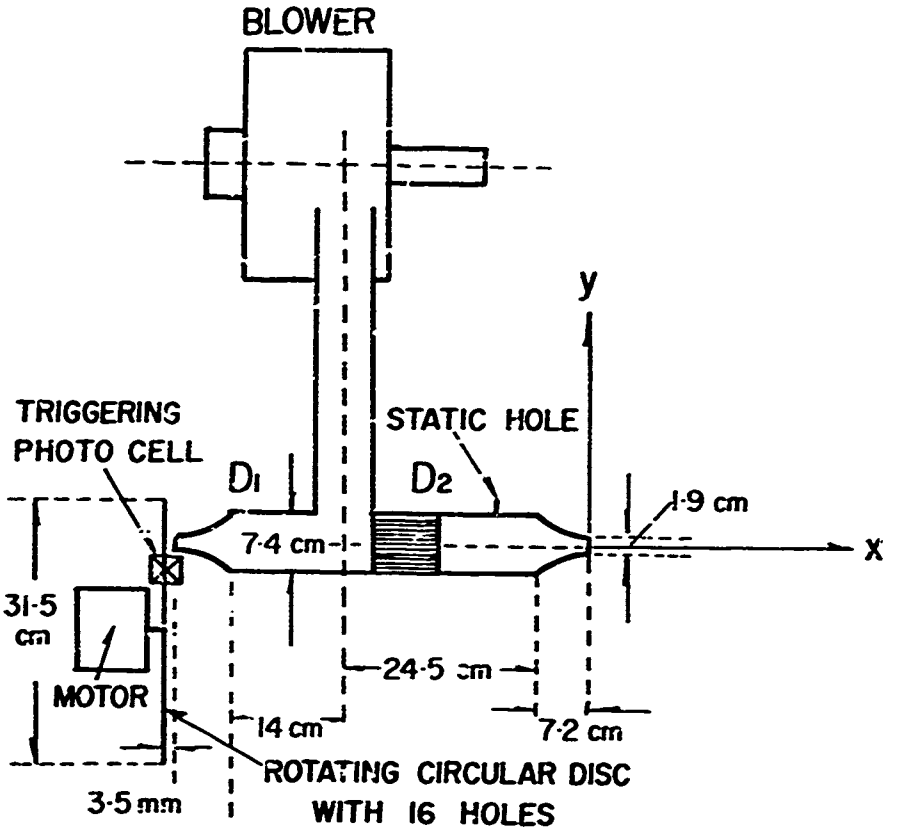

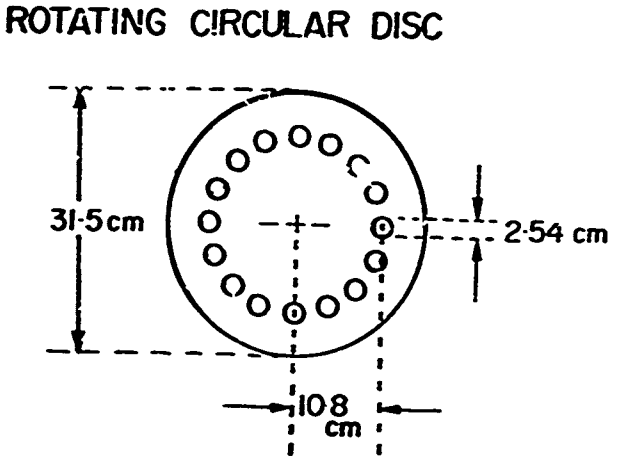

Fig. 1 Pulsating flow generator

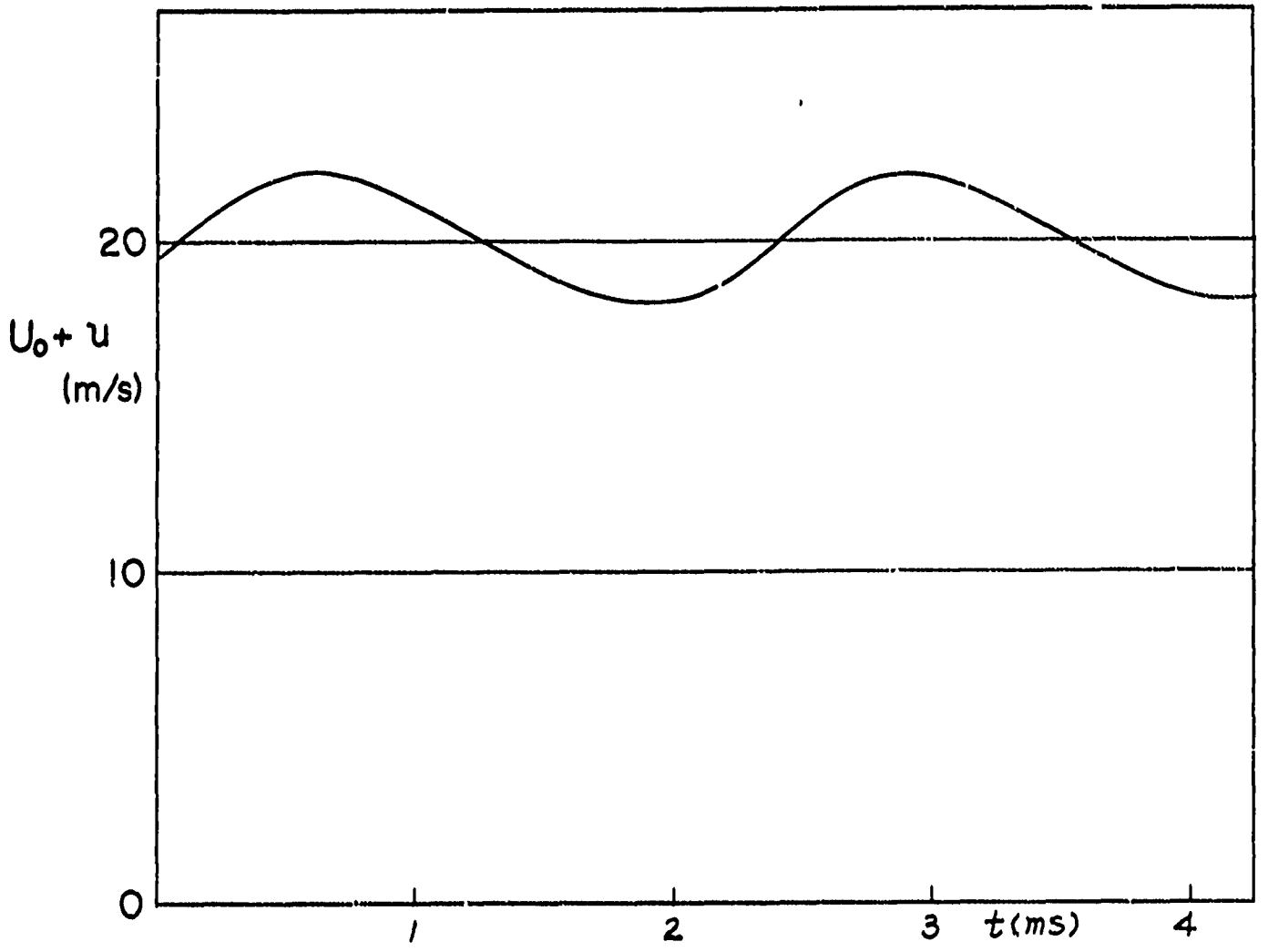

Fig. 2 Pulsating velcoity of the jet at x = 6 cm, pulsating frequency 450 Hz

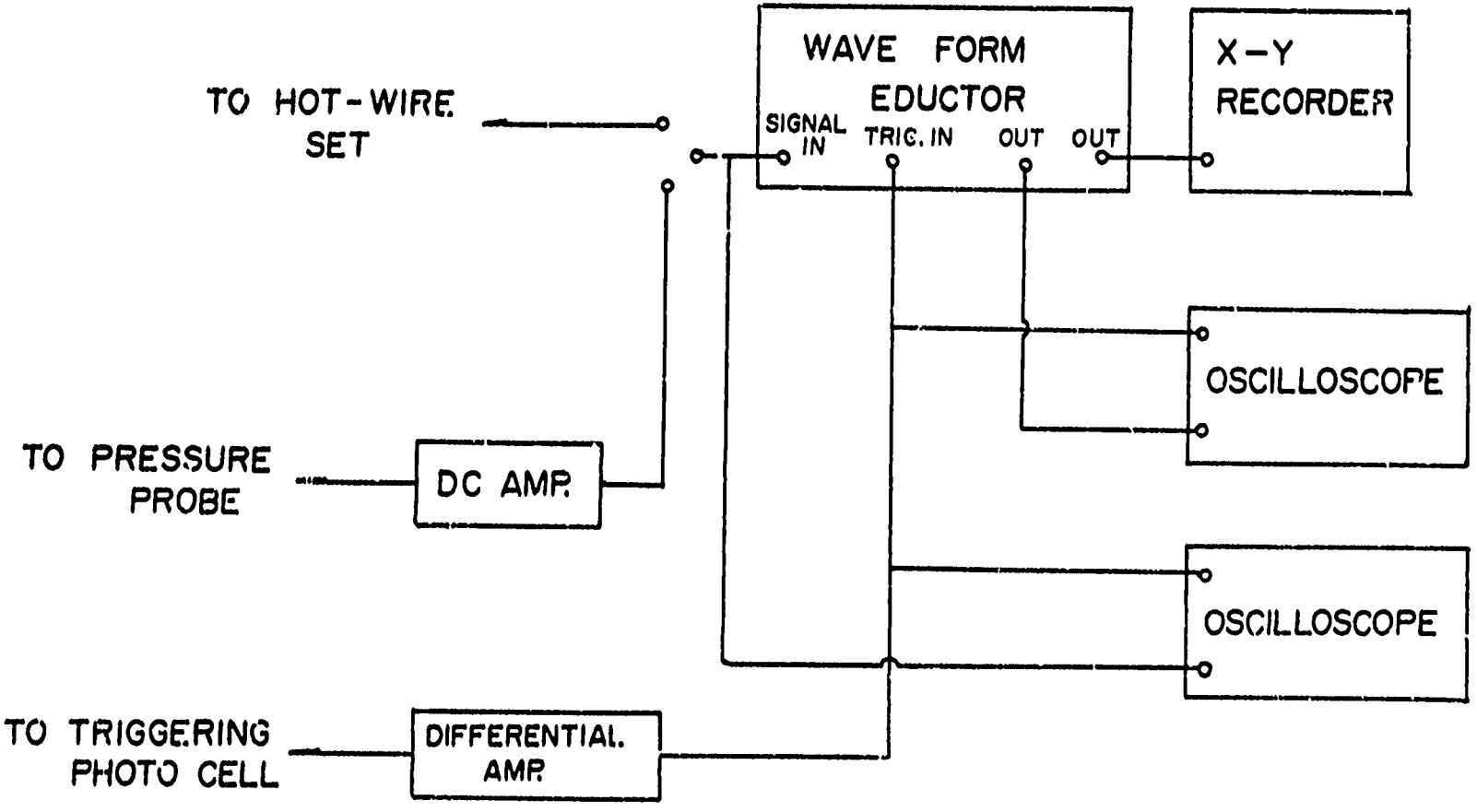

Fig. 3 Schematic diagram of data acquisition

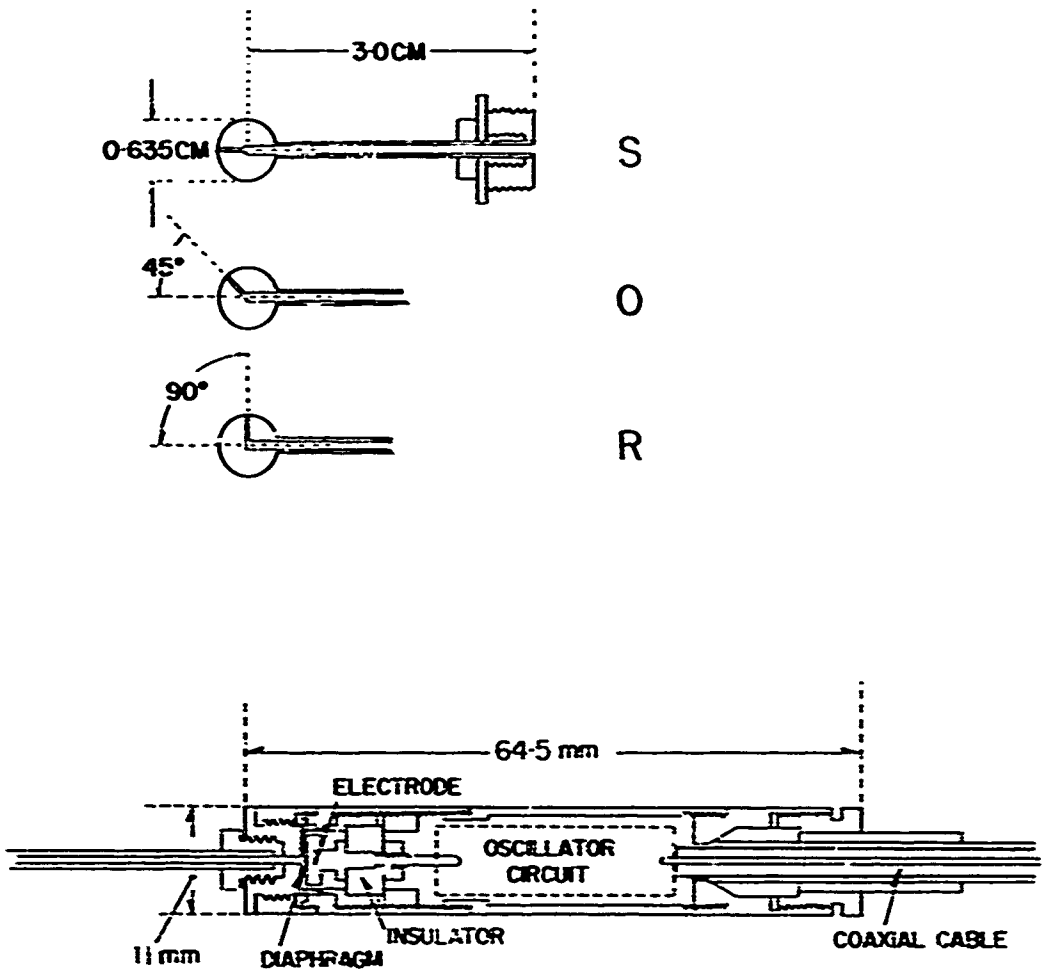

Fig. 4 Three sphere models and condenser microphone

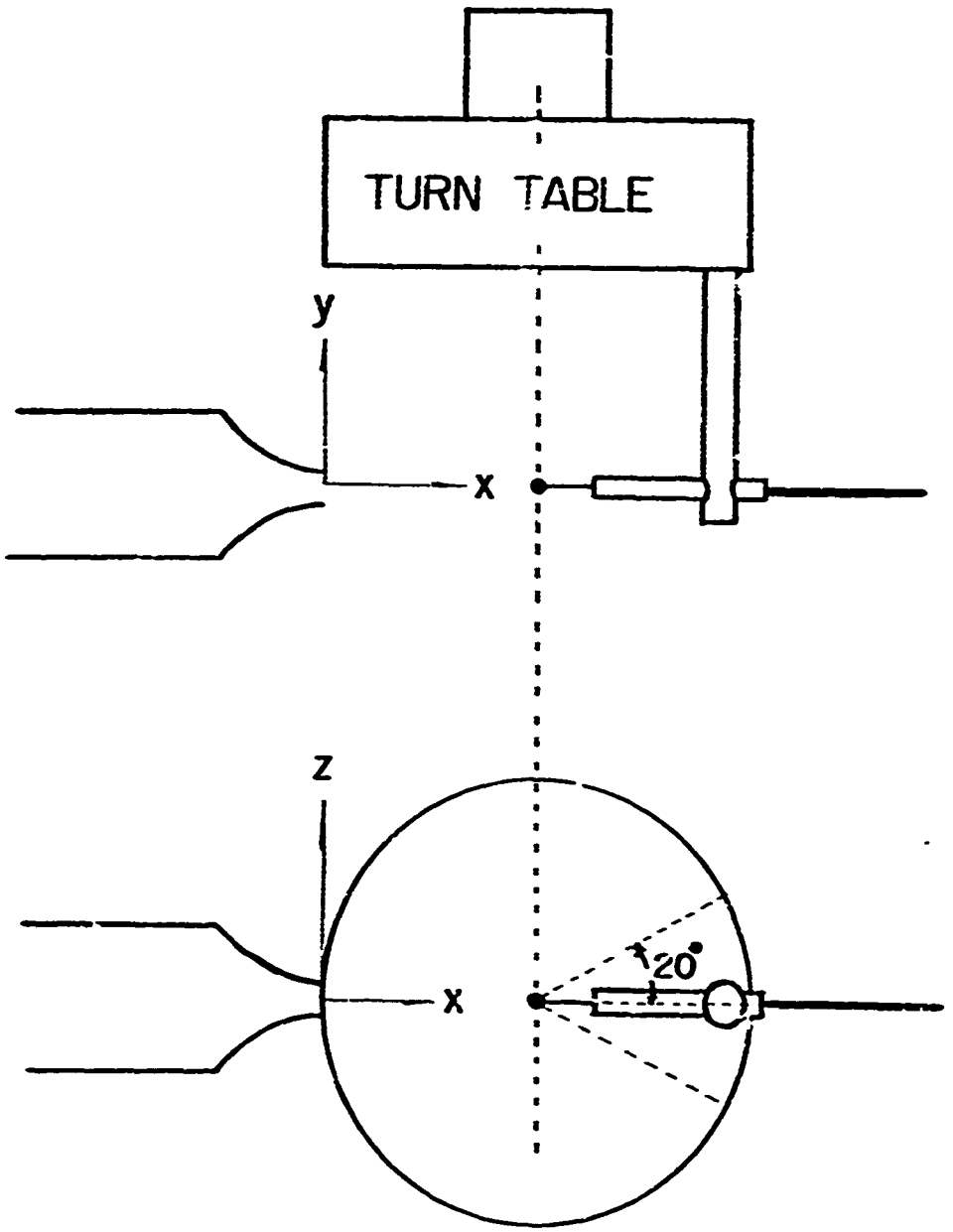

Fig. 5 Rotation of the model

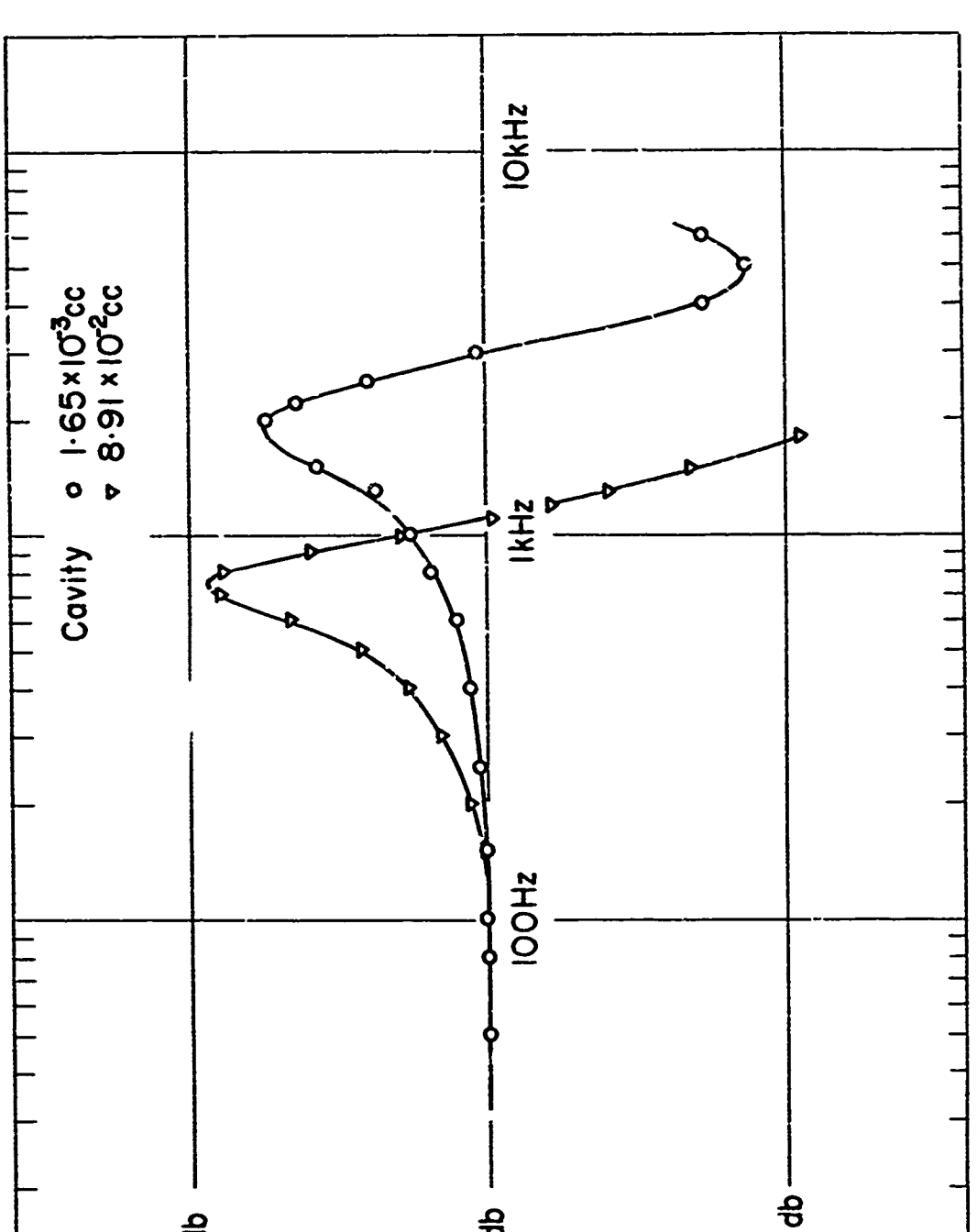

Fig. 6 Calculated frequency response of microphone with cavities

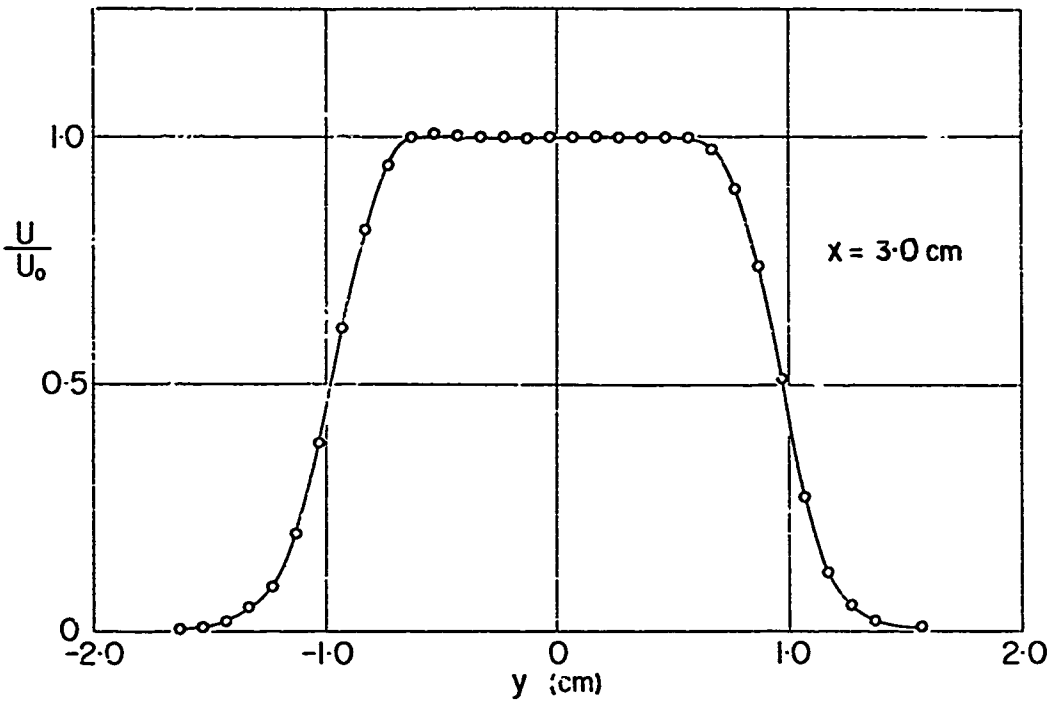

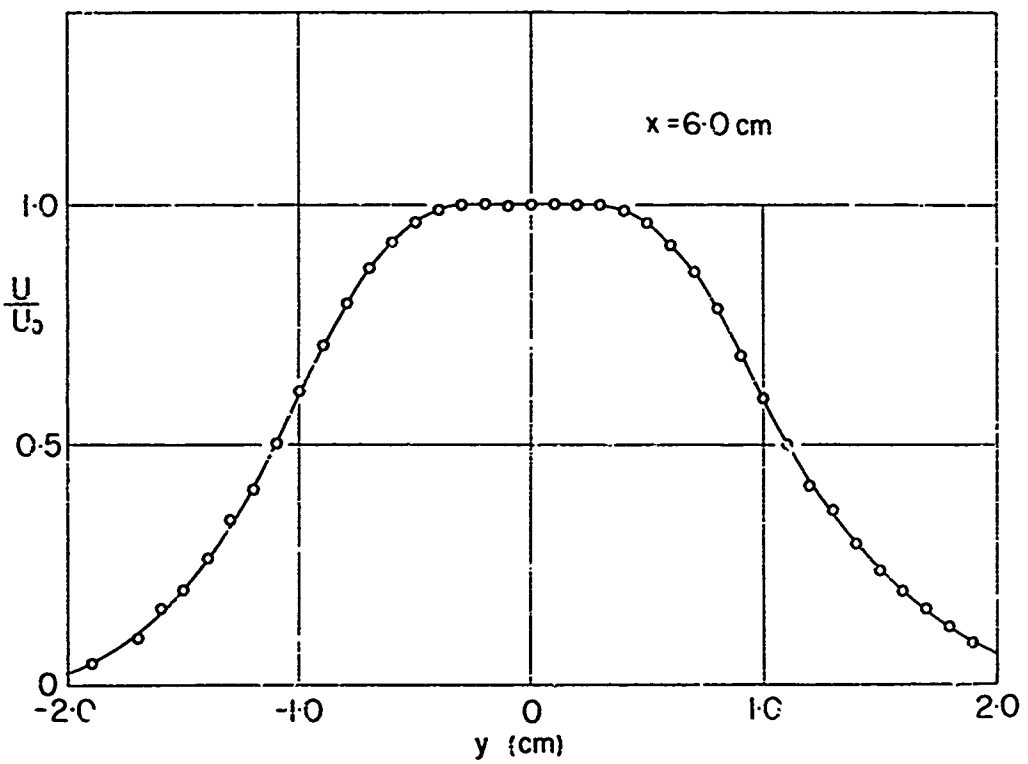

Fig. 7 Mean velocity distribution of steady jet at x = 3 and 6 cm.

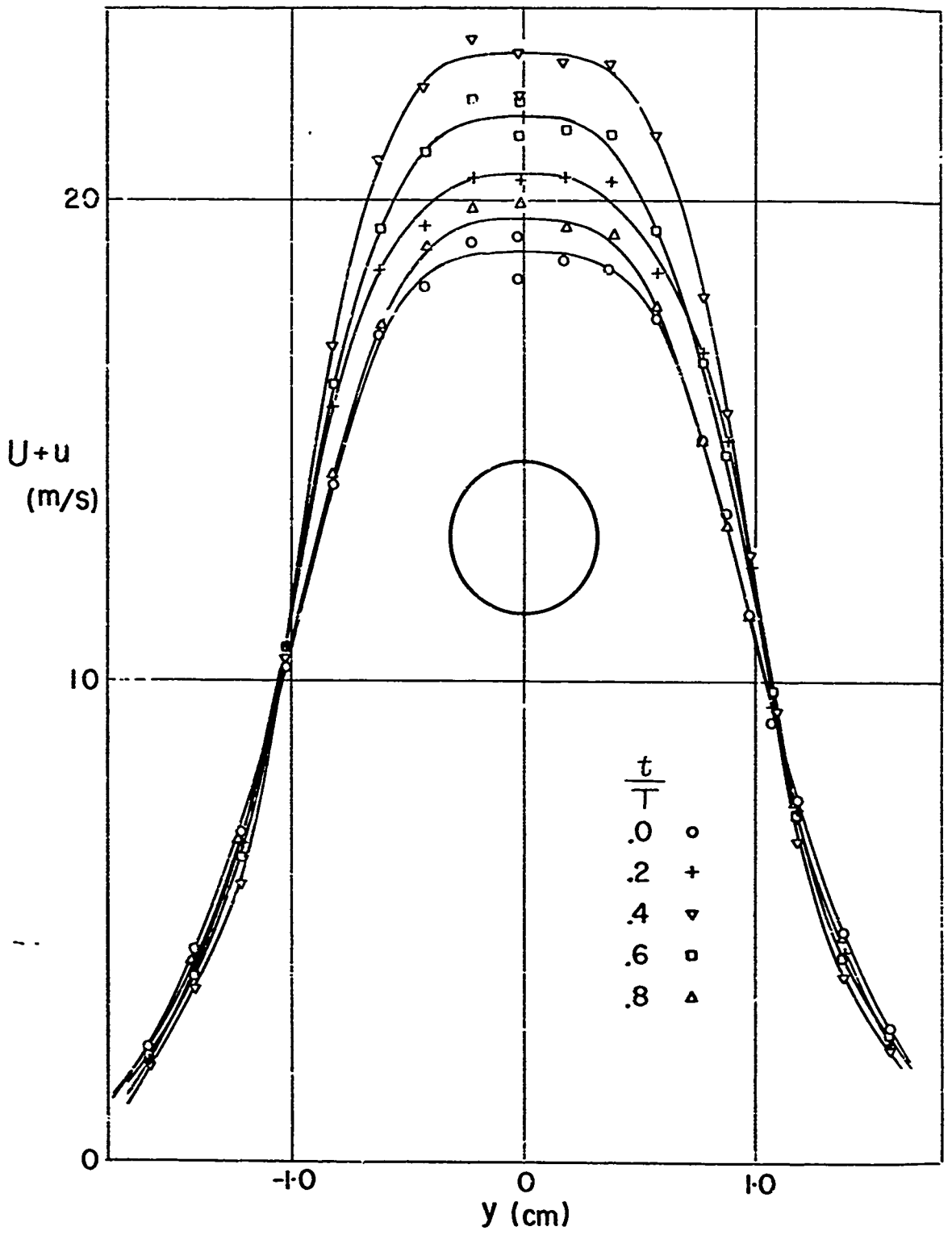

Fig. 8 Instantaneous velocity distribution of pulsating jet at x = 5 cm, f = 450 H_z

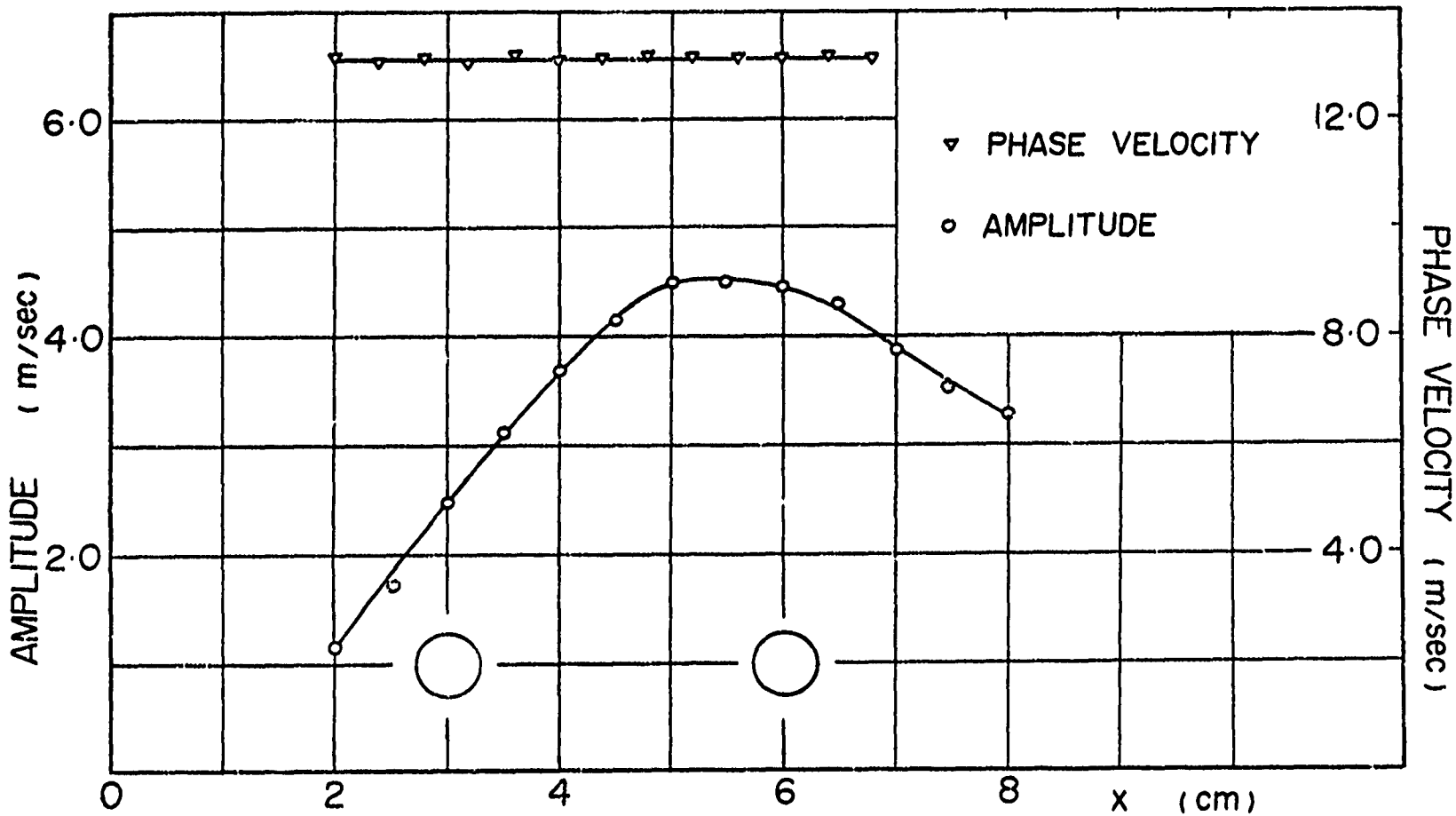

Fig. 9 Pulsating velocity amplitude and phase velocity along the centerline of jet at f = 450 Hz

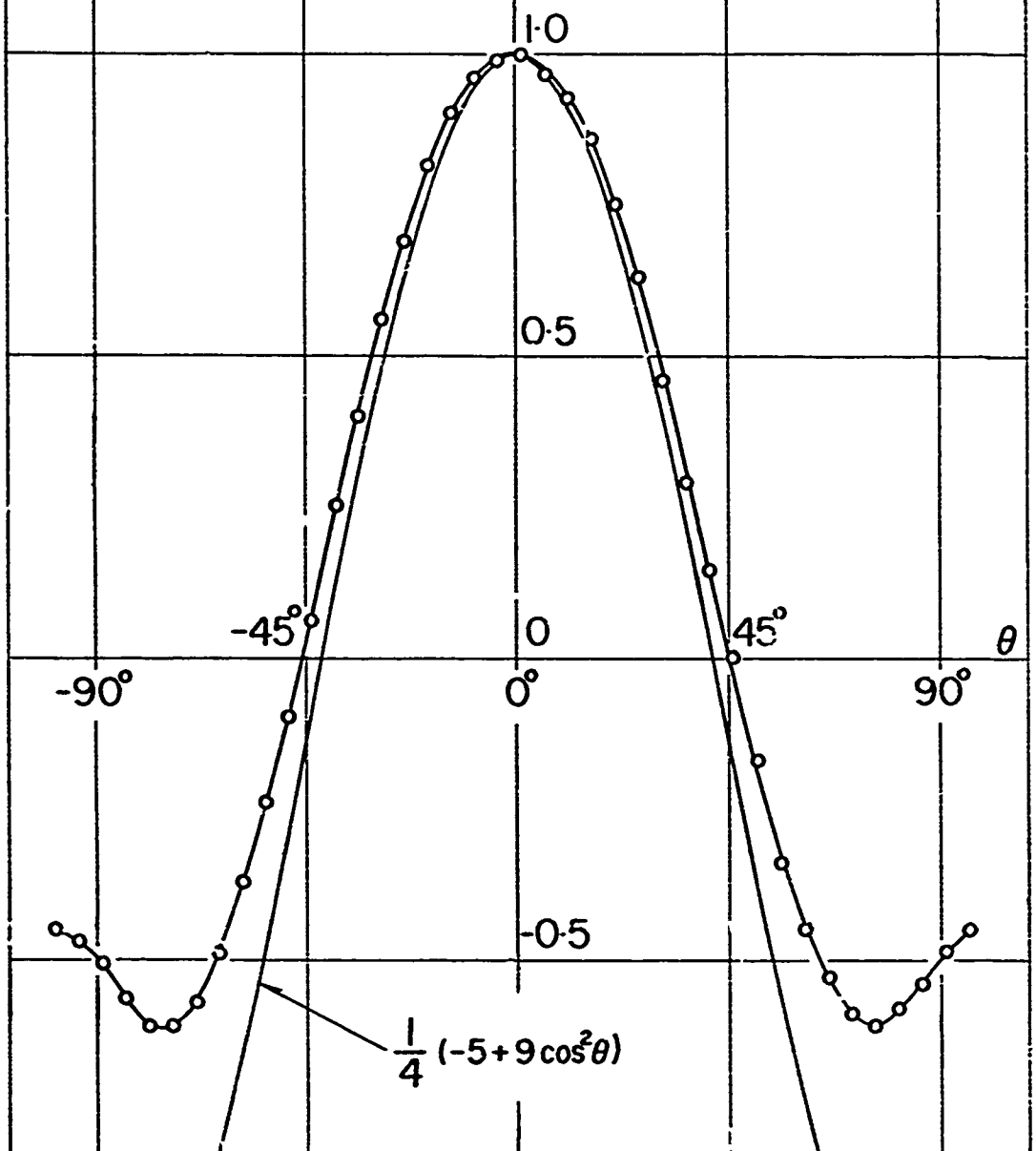

Fig. 10 Pressure distribution around the sphere ir steady flow (solid line indicates inviscid theory)

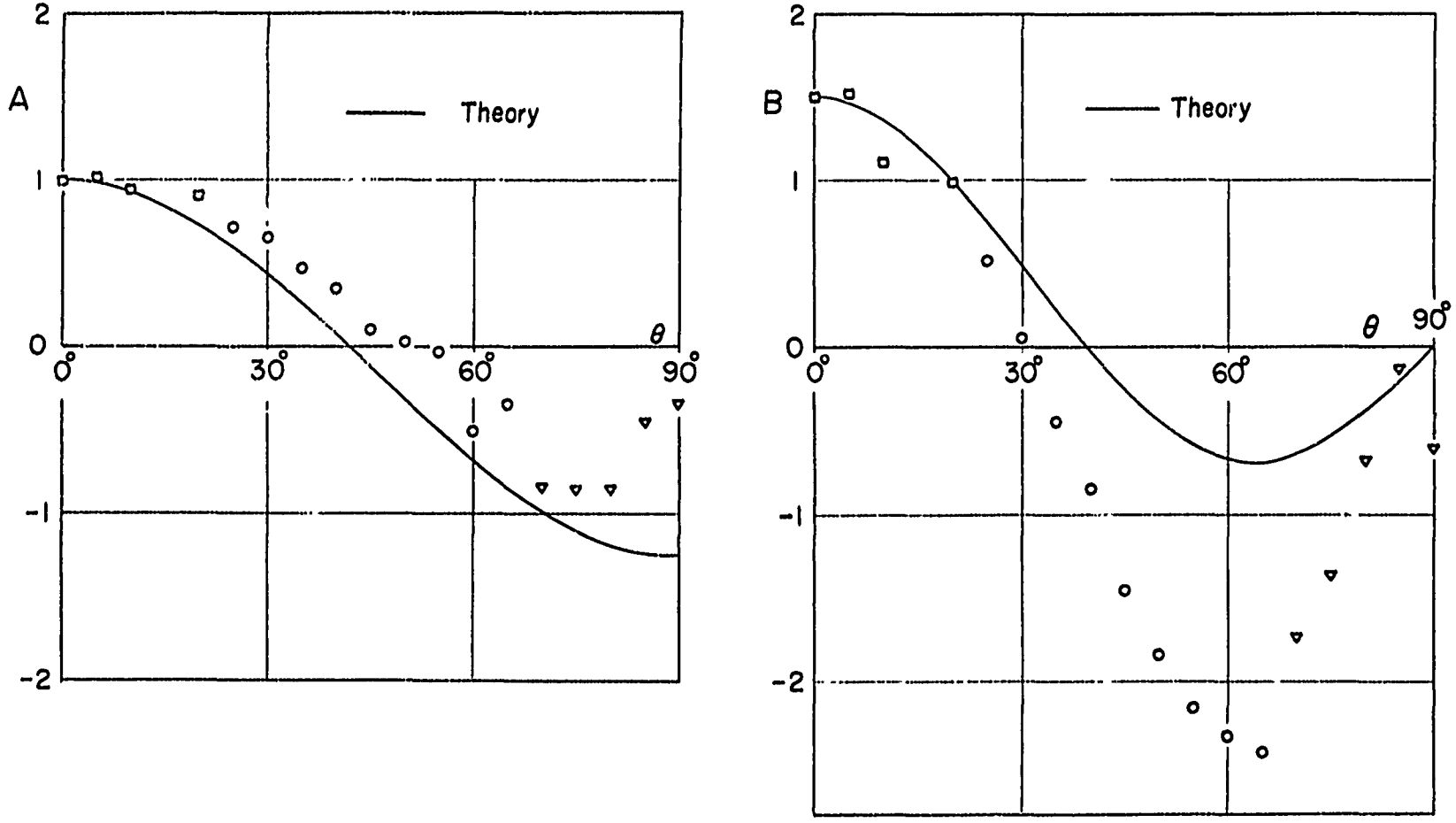

Fig. 11 Coefficients A and B at x = 3 cm, f= 450 Hz

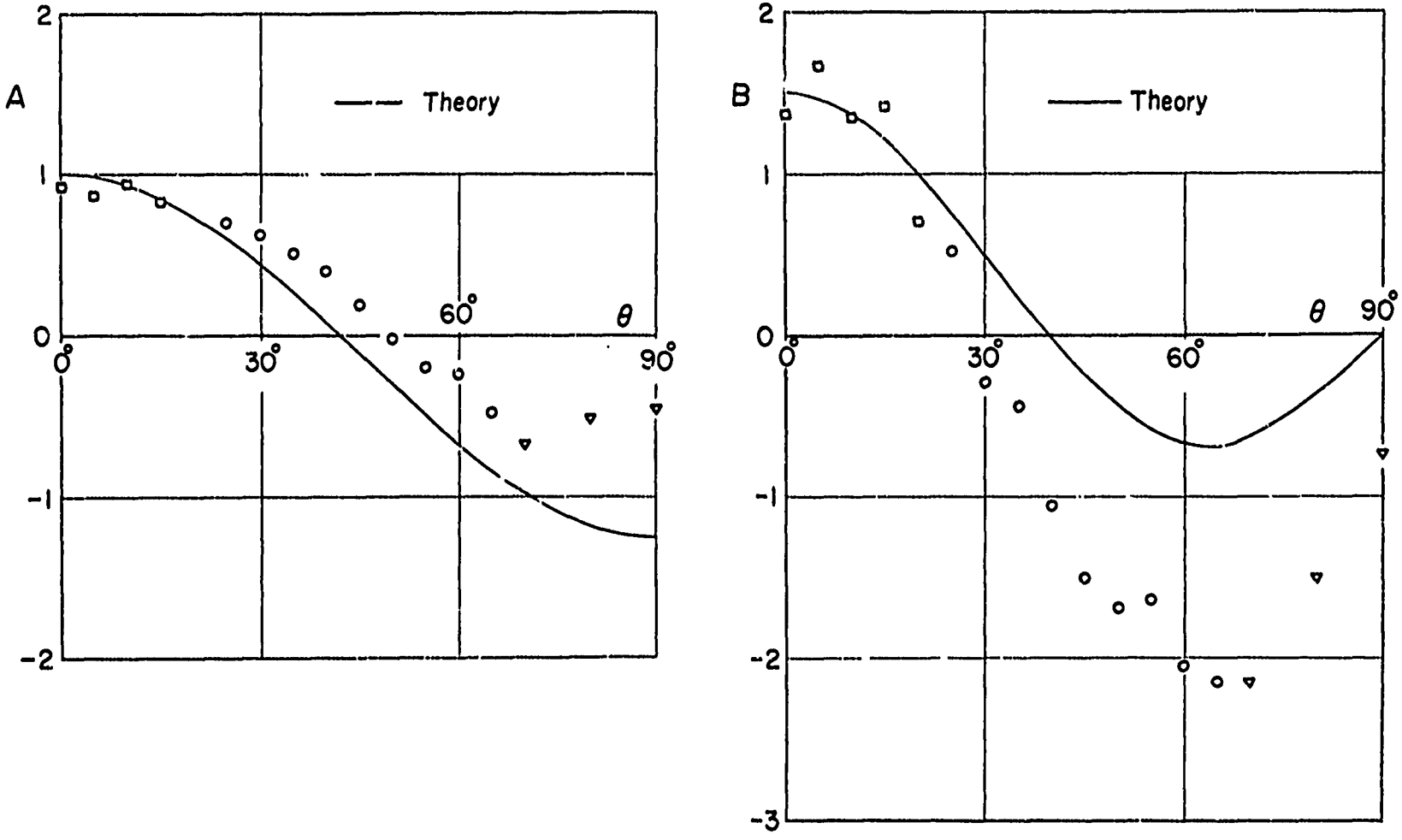

Fig. 12 Coefficients A and B at x = 3 cm, f = 300 Hz

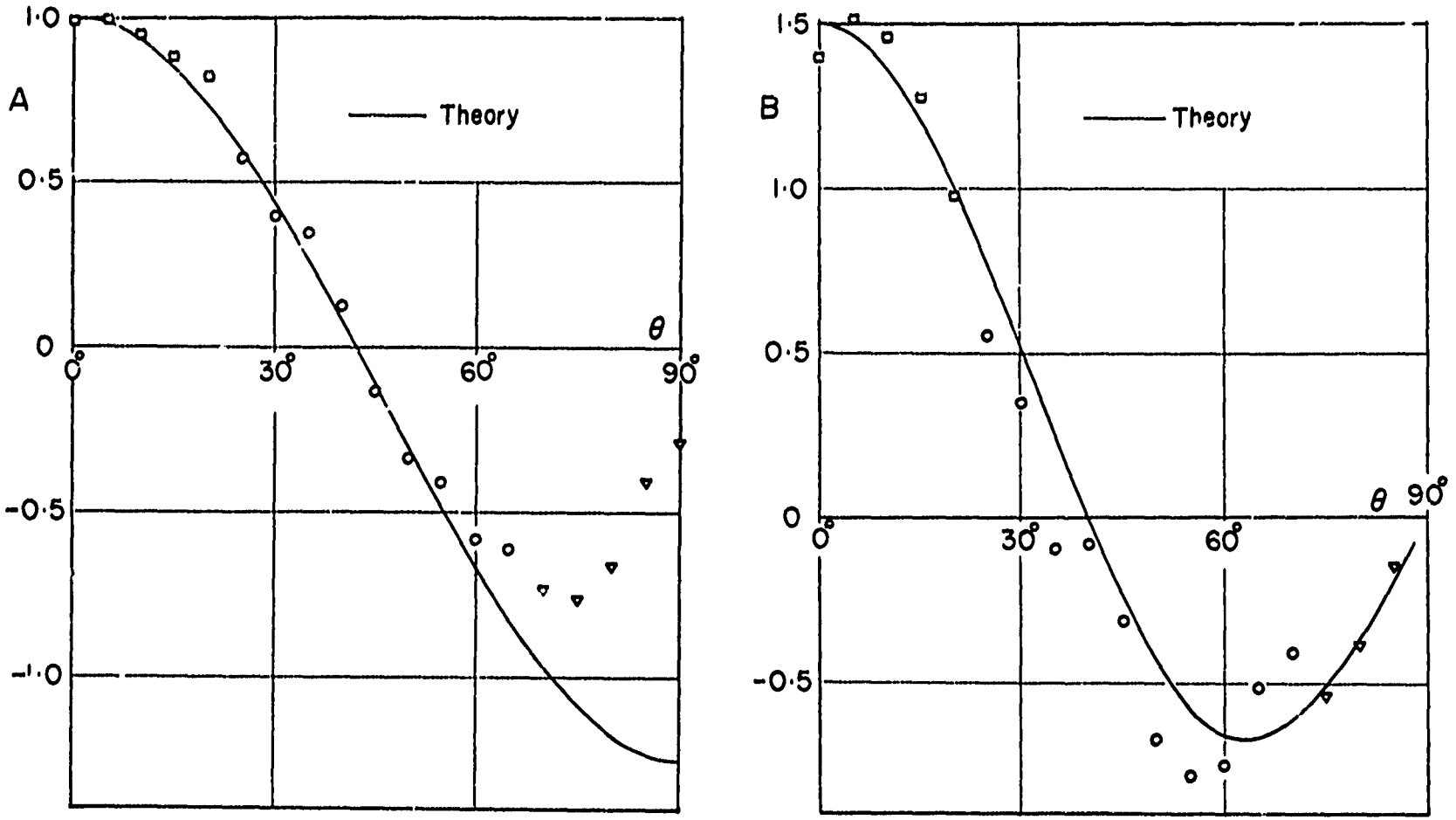

Fig. 13 Coefficients A and B at X = 6 cm, f = 350 Hz

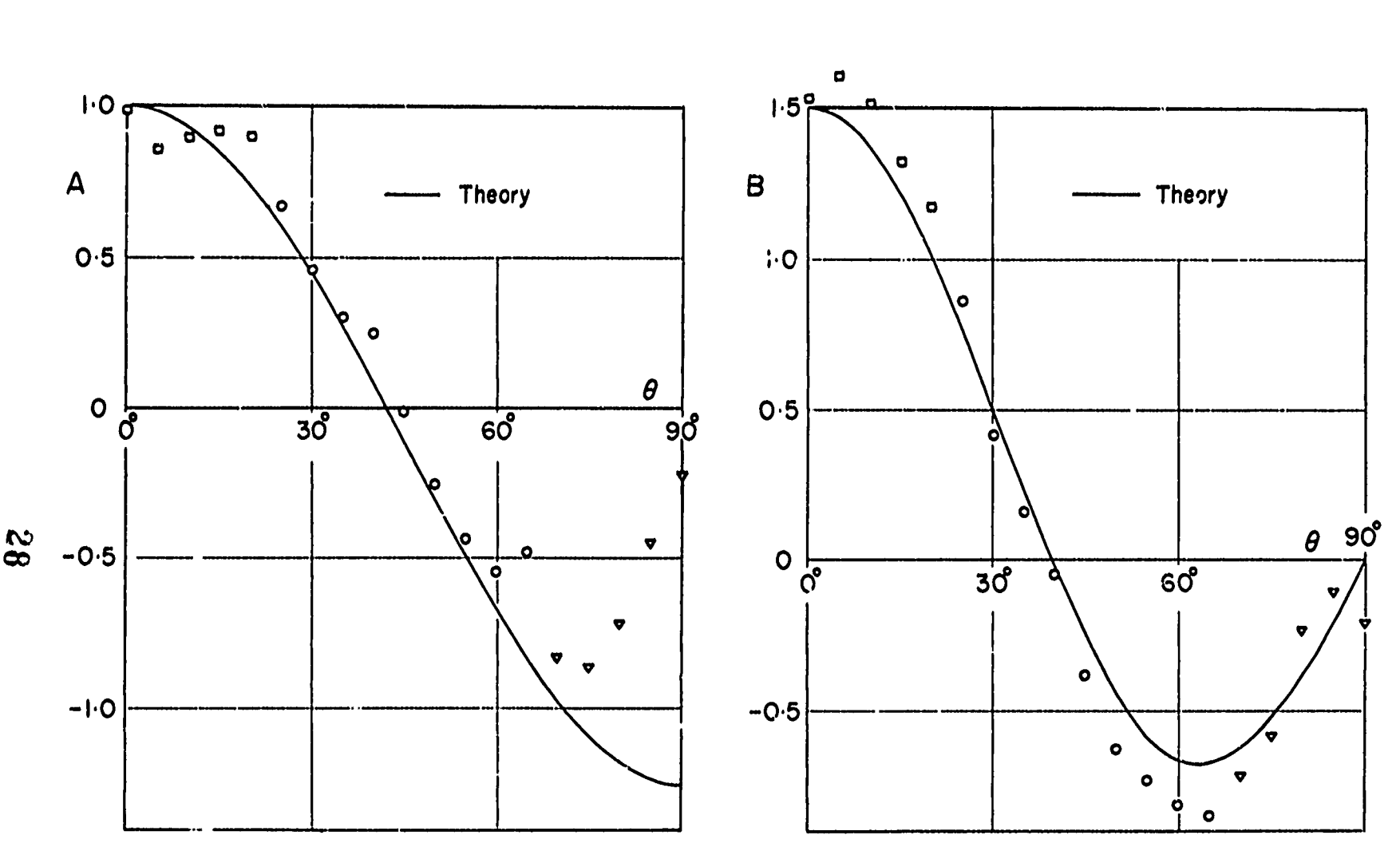

Fig. 14 Coefficients A and B at X = 6 cm, f = 450 Hz

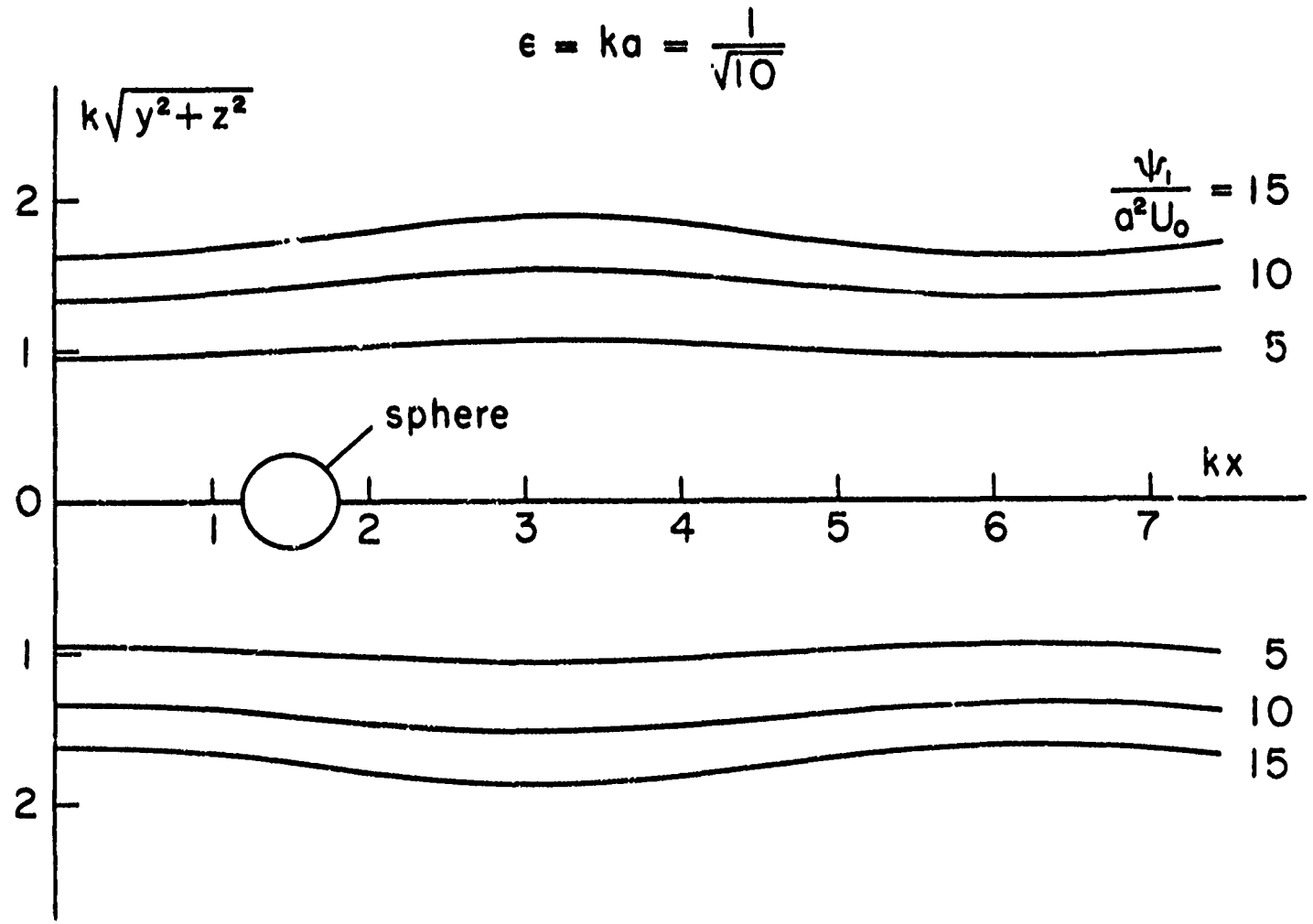

Fig. 13 Streamlines of theoretical model for ϵ = ka = 1 10